Materials Today Bio 13 (2022) 100190

Contents lists available at ScienceDirect

Materials Today Bio

journal homepage: www.journals.elsevier.com/materials-today-bio

Microtissues from mesenchymal stem cells and siRNA-loaded cross-linked gelatin microparticles for bone regeneration

Sandra Hinkelmann [a], Alexandra H. Springwald [a], Annett Starke [a], Hermann Kalwa [b], Christian Wölk [a], Michael C. Hacker [a,c], Michaela Schulz-Siegmund [a,*]

[a] Institute of Pharmacy, Pharmaceutical Technology, Faculty of Medicine, University of Leipzig, Germany
[b] Rudolf-Boehm-Institute for Pharmacology and Toxicology, Faculty of Medicine, University of Leipzig, Leipzig, Germany
[c] Institute of Pharmaceutics and Biopharmaceutics, Heinrich Heine University, Düsseldorf, Germany

ARTICLE INFO

Keywords:
Gelatin microparticles
hMSC
Microtissues
Chordin
siRNA
Osteogenic differentiation

ABSTRACT

The aim of this study was the evaluation of cross-linked gelatin microparticles (cGM) as substrates for osteogenic cell culture to assemble 3D microtissues and their use as delivery system for siRNA to cells in these assemblies.

In a 2D transwell cultivation system, we found that cGM are capable to accumulate calcium ions from the surrounding medium. Such a separation of cGM and SaOS-2 cells consequently led to a suppressed matrix mineral formation in the SaOS-2 culture on the well bottom of the transwell system. Thus, we decided to use cGM as component in 3D microtissues and get a close contact between calcium ion accumulating microparticles and cells to improve matrix mineralization.

Gelatin microparticles were cross-linked with a *N,N*-diethylethylenediamine-derivatized (DEED) maleic anhydride (MA) containing oligo (pentaerythritol diacrylate monostearate-*co*-*N*-isopropylacrylamide-*co*-MA) (oPNMA) and aggregated with SaOS-2 or human mesenchymal stem cells (hMSC) to microtissue spheroids. We systematically varied the content of cGM in microtissues and observed cell differentiation and tissue formation. Microtissues were characterized by gene expression, ALP activity and matrix mineralization. Mineralization was detectable in microtissues with SaOS-2 cells after 7 days and with hMSC after 24–28 days in osteogenic culture. When we transfected hMSC via cGM loaded with Lipofectamine complexed chordin siRNA, we found increased ALP activity and accelerated mineral formation in microtissues in presence of BMP-2. As a model for positive paracrine effects that indicate promising *in vivo* effects of these microtissues, we incubated pre-differentiated microtissues with freshly seeded hMSC monolayers and found improved mineral formation all over the well in the co-culture model. These findings may support the concept of microtissues from hMSC and siRNA-loaded cGM for bone regeneration.

1. Introduction

Current strategies to support repair of critical size bone defects include implantation of bone graft materials such as autografts, allografts, xenografts, and synthetic biomaterials, with autologous bone being the gold standard for such therapies [1]. The risk of donor site morbidity and pathologies as well as limited availability, however, remain problematic issues for autografts. Allografts are an alternative but have been associated to immune rejection and disease transmission [2]. Therefore, biomaterials for bone replacement are being progressed, especially substances that could enhance fracture healing and bone regeneration.

In this study, we combined gelatin as cell-adhesive biomaterial with an autologous-based approach for bone tissue engineering. Human mesenchymal stem cells (hMSC) having the capacity to differentiate to the osteogenic, chondrogenic and adipogenic lineage are widely applied in engineering of bone or cartilage. The expansion of hMSC in a classical two-dimensional (2D) cell culture system, however, requires a proteolytic treatment, e.g. with trypsin, that leads to the destruction of important matrix proteins and cellular interactions. The cultivation of cells in a three-dimensional (3D) environment offers the advantage that the cell-cell contacts are preserved, resulting in enhanced biological functions or differentiation of cells and more efficient production of extracellular matrix proteins than in single cells [3].

* Corresponding author.
E-mail address: schulz@uni-leipzig.de (M. Schulz-Siegmund).

https://doi.org/10.1016/j.mtbio.2021.100190
Received 15 September 2021; Received in revised form 20 November 2021; Accepted 11 December 2021
Available online 17 December 2021

Nevertheless, the cultivation of cell aggregates is often associated with problems, such as necrotic core formation due to lacking supply with oxygen and nutrients caused by consumption in the densely packed cell layers and gradient formation to the inner cell layers [4]. The incorporation of hydrogel materials, e.g. gelatin microparticles, into the aggregate reduces the number of cells per volume and supports the supply of cells in the inner part by improved diffusion exchange of nutrients and oxygen though the hydrogel matrix [5,6].

The combination of 3D cell culture and microparticles, here addressed as microtissues, could form the basis of building blocks for tissue reconstruction. Gelatin microparticles were cross-linked (cGM) with an anhydride containing oligomer developed in our group [7–9] and incorporated into SaOS-2 or hMSC aggregates (Fig. 1). Applying a cross-linking strategy with gelatin is necessary to achieve and control mechanical stabilities of the particles at physiological conditions. Utilizing our specific anhydride-containing oligomeric cross-linker is particularly interesting as the cross-linking strategy allows for a partial and straight-forward, covalent modification with small amines to modify physico-chemical or biological properties. In addition, our cross-linking strategy has been shown to be biocompatible and the resulting predominantly negatively charged matrices may mimic properties of natural extracellular matrix and support matrix mineralization via calcium ion complexation by carboxylate groups [10–12].

A microtissue based regenerative approach also enables cells to be treated *ex vivo* before microtissues are formed, or indirectly upon microtissue formation with siRNA-carrying cGM, which could act as a

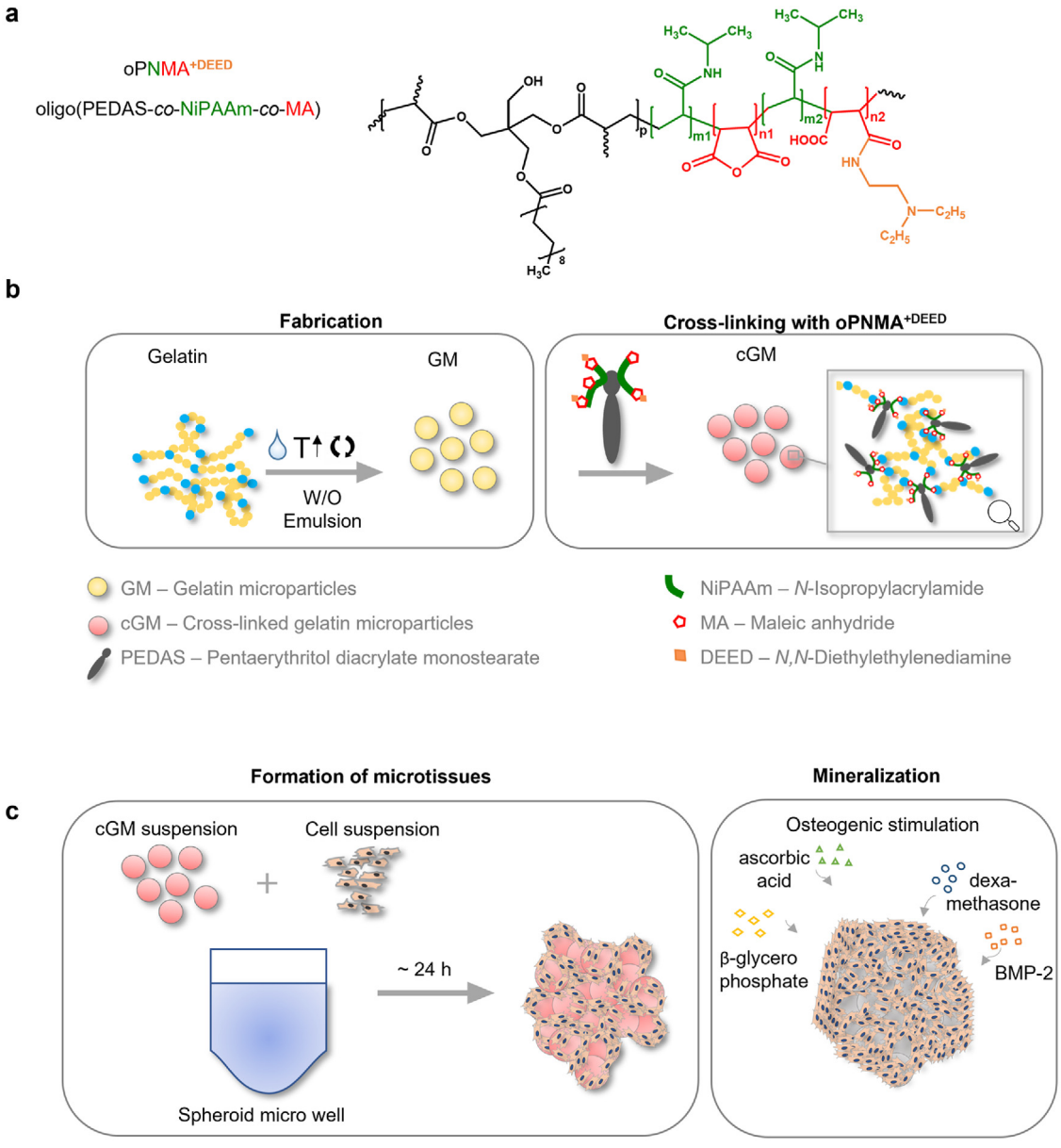

Fig. 1. Graphical outline of cross-linker, fabrication, and cross-linking of gelatin microparticles and microtissues. (a) Chemical structure of *N*,*N*-diethylethylenediamine-derivatized (DEED) oligo (PEDAS-co-NiPAAm-co-MA) cross-linker. (b) Fabrication of gelatin microparticles with emulsion technique and cross-linking reaction with DEED-oPNMA. Cross-linked hydrogel network with incorporated DEED-oPNMA. Gelatin was covalently cross-linked by non-derivatized maleic anhydrides (MA) with amide bonds. The derivatization of the MA with DEED leads to the incorporation of positive charges to the mainly negatively charged cross-linked network. (c) Experimental procedure to obtain mineralized microtissues based on cross-linked gelatin microparticles (cGM) and SaOS-2 or hMSC. 24 h after seeding, cells were stimulated osteogenic medium and started mineralization after 7 days (SaOS-2 cells) or 24 days (hMSC).

drug delivery system and may allow a continuous stimulation to develop functional tissue. The BMP-2 antagonist chordin was chosen as a promising target for our system. We and others have shown before that silencing of chordin in combination with BMP-2 supplementation could enhance osteogenic differentiation and accelerate mineralization in osteogenic cultures of hMSC [13–16].

In this study, hMSC were transfected with chordin siRNA complexed by Lipofectamine® RNAi/MAX directly before mixing with cGM or indirectly by siRNA releasing cGM. Gene expression, ALP (Alkaline phosphatase) activity and calcium content were analyzed. We demonstrate that ALP activity and calcium content were positively influenced by an initial transfection of cells as well as a prolonged cGM-based indirect transfection with chordin siRNA and simultaneous stimulation by BMP-2. As proof-of-concept with regard to the application in bone defects, we could show that differentiated microtissues are able to induce and accelerate the mineralization of freshly seeded hMSC in co-culture.

2. Methods

2.1. Particle fabrication

Fabrication and cross-linking of gelatin microparticles with *N,N*-diethylethylenediamine (DEED)-derivatized oligo (pentaerythritol diacrylate monostearate-*co*-*N*-isopropylacrylamide-*co*-maleic anhydride) (oPNMA) was performed according to previously described protocols [7–9]. Briefly, 5 g gelatin (from bovine skin, type B, 225 Bloom, Sigma Aldrich, Seelze, Germany) was dispersed in 45 ml water and heated up to 60 °C to obtain a homogenous solution. Gelatin solution was added dropwise to 200 mL of Kollisolv® MCT (Caelo, Hilden, Germany) at 60 °C and emulsified with an over-head stirrer at 800 rpm for 10 min. Consequently, the W/O emulsion was cooled down with ice and stirred for 30 min. For particle hardening, 100 ml of cold acetone was added, and the emulsion was stirred for another hour. Microparticles were washed with acetone and dried before cross-linking with DEED-derivatized oPNMA-7.5 (7.5 refers to the molar ratio of MA to pentaerythritol diacrylate monostearate during oPNMA synthesis; for more details please refer to Ref. [9]) and a gelatin to cross-linker-ratio of 1:2 (these particles are addressed as oPNMA 7.5–10% as this ratio correlates with an oPNMA concentration in the acetonic solution of 10% (w/v)). The cross-linker solution was prepared starting with the covalent derivatization of the anhydride-containing oligomer with the heterobifunctional diamine DEED. To this end, 116 µl DEED (Sigma Aldrich, Seelze, Germany) was added to 2 g of oPNMA dissolved in 18 ml acetone and incubated for 2 h. The amount of DEED was calculated to obtain theoretical derivatization of 25% of intact anhydride groups in oPNMA. The solution of derivatized DEED-oPNMA was added to microparticles dispersed in 2 ml acetone. Water (10 ml) was added and stirred at 800 rpm for 4 h. Subsequently, cross-linked gelatin microparticles (cGM) were repeatedly washed with acetone and vacuum-dried overnight.

2.2. Particle characterization

The cross-linked particles were characterized with regard to the degree of cross-linking, the particle size distribution and the phosphate buffered saline (PBS) uptake capacity.

The degree of cross-linking was assessed by a standard colorimetric assay (TNBS assay) which determines the amount of free amine groups that were not consumed by the cross-linking reaction. Detailed instructions are provided in previously published protocols [7,17]. The absorbance was measured spectrophotometrically at 346 nm (Genesys, Thermo Scientifc™, Germany). The degree of cross-linking was calculated by comparing the amount of free amine groups of cross-linked and non-cross-linked particles.

The average particle size of non-swollen particles was analyzed in isopropyl alcohol by laser diffraction (Mastersizer 3000 with Hydro SV dispersion unit, Malvern Panalytical GmbH, Kassel, Germany). The dispersion was stirred at 2000 rpm for 5 min before the particle size distribution was obtained from the diffraction signals using the Fraunhofer approximation. To determine the swollen average particle size, particles pre-swollen in PBS overnight were analyzed in PBS. The results were expressed as the volume moment mean (D [3,4], De Brouckere Mean Diameter).

The factor of PBS uptake is important for the post-fabricated loading of cGM with API by swelling. To ensure that all of the API-containing medium is taken up by the particles, the volume of the loading medium was calculated using 80% of this factor. The determination was carried out using a gravimetric method according to the literature [18].

2.3. Cell culture

SaOS-2 were cultivated in culture medium (CM) McCoys 5A (Sigma Aldrich, Seelze, Germany), 15% (v/v) fetal bovine serum albumin (FBS, Biochrome, Berlin, Germany) and 1% (v/v) Penicillin/Streptomycin (P/S, Sigma Aldrich, Seelze, Germany). For osteogenic differentiation, cells were seeded in a well plate with a density of $3\bullet10^4$ cells/cm^2 in CM. After 24 h cells were stimulated with osteogenic medium (OM/OM^{+BMP-2}) based on DMEM (Sigma Aldrich, Seelze, Germany), 10% (v/v) FBS, 1% (v/v) P/S, 100 nM Dexamethasone (Sigma Aldrich, Seelze, Germany), 285 µM Ascorbic acid (Sigma Aldrich, Seelze, Germany), 10 mM β-Glycerophosphate disodium salt hydrate (Sigma Aldrich, Seelze, Germany) and with/without 100 ng/ml bone morphogenetic protein (BMP-2, R&D Systems, Wiesbaden, Germany). DMEM with 10% FBS and 1% P/S served as control. Human mesenchymal stem cells (hMSC, Lonza, Basel, Switzerland) were cultivated in culture medium (CM) DMEM, 10% (v/v) FBS, 1% (v/v) MEM non-essential Amino Acid Solution (AA, Sigma Aldrich, Seelze, Germany) and 1% (v/v) P/S. Osteogenic differentiation was performed in DMEM, 10% (v/v) FBS, 1% (v/v) AA, 1% (v/v) P/S, 100 ng/ml Dexamethasone, 50 µg/ml Ascorbic acid, 10 mM β-Glycerophosphate and with/without 100 ng/ml BMP-2.

2.4. Cell viability

Analysis of cytotoxicity was performed in a NUNC® carrier plate transwell system (insert position: medium). Different amounts of cGM (4 mg, 10 mg, 20 mg) were swollen and suspended in 1.5 ml Mc Coys medium with 15% FBS and 1% P/S. Particle suspension was added in the upper chamber to 24 h pre-seeded SaOS-2 cells ($6\bullet10^4$ cells/Well) and gently shaken on orbital shaker (70–80 rpm) for 30 min at 37 °C and 5% CO_2. Samples were incubated under static conditions for further 48 h. Cell viability was investigated by ROTITEST® Bio Analysis (Carl Roth, Karlsruhe, Germany) in accordance with the manufacturer instructions. Supernatant of incubated samples were collected and measured in a 96 well plate with a Tecan infinite m200 (Tecan, Männedorf, Switzerland) plate reader and normalized to non-treated control.

2.5. Calcium quantification

Analysis of calcium absorption through cGM was performed in a NUNC® carrier plate transwell system (insert position: medium). 5 mg of cGM were added in the upper chamber to 24 h pre-seeded SaOS-2 cells ($6\bullet10^4$ cells/Well) and gently shaken on orbital shaker (70–80 rpm) for 30 min at 37 °C and 5% CO_2. Samples were incubated under static conditions for further 24 h and medium was changed to OM. Supernatants were collected in reaction tubes. Calcium absorption was measured by Calcium AS FS (Diasys, Holzheim, Germany) according to the manual. Deficits of calcium in supernatants were calculated as absorption by the cGM.

For another experiment, calcium concentration was increased up to 15% to compensate for absorbed calcium. To analyze mineralization of cells and microtissues, medium was removed and samples were carefully washed with warm PBS (37 °C). For cell lysis, 0.5 N HCl (Th. Geyer, Berlin, Germany) was added, and samples were incubated at room

Table 1
The sense and antisense sequences of chordin siRNA.

siRNA	SEQUENCE (5′-3′)	
si**CHORDIN**	Sense	G.G.U.G.C.A.C.A.U.A.G.C.C.A.A.C.C.A.A.dT.dT
	Antisense	U.U.G.G.U.U.G.G.C.U.A.U.G.U.G.C.A.C.C.dT.dG

temperature (RT) for 24 h during shaking. Afterwards samples were transferred to reaction tubes, incubated in an ultrasonic bath for 2 h and shaken for further 12 h at RT. Samples were measured as described above and calcium content was calculated relative to DNA content per well.

2.6. pH measurement

5 mg of cGM were swollen in 40 μl of OptiMEM® for 30 min at 4 °C, resuspended in 1.5 ml OptiMEM® and transferred to a well plate. Particle suspension was gently shaken on orbital shaker (70 rpm) for 30 min at 37 °C and 5% CO_2. Samples were incubated under static conditions for 24 h. Measurement of pH was performed in supernatant with pH electrode (Thermo Scientific™, Germany).

2.7. 3D culture with cGM and cells as microtissues

To obtain 3D cell-microparticle-spheroids, SaOS-2 cells and hMSC were cultured in CM until 90% confluency and detached with Trypsin/EDTA. 100 μl of single cell suspension (10^5 cells•ml^{-1}) were added to 100 μl of cGM suspension (0.21, 0.64 or 8.3 mg•ml^{-1}) in OptiMEM® supplemented with 10% FBS in one well of a low adhesion 96 well plate (Spheroid microplate, Corning, NY, USA) and gently shaken for 1–3 s. Based on the calculated surface area of cGM (calculated using the determined diameter), we decided on ~ 100 (0.021 mg) and ~300 (0.064 mg) particles/10^4 cells in one spheroid micro well [6,19]. The ratio of 0.83 mg cGM/10^4 cells was chosen because it corresponds to the amount used in 2D transwell experiments. Samples were incubated at 37 °C and 5% CO_2. For osteogenic differentiation medium was changed 24 h after treatment with cGM to OM or OM^{+BMP-2}. Medium change or washing steps were performed partially twice by careful removing of 200 μl used medium and replacing by 200 μl fresh medium.

2.8. Transfection of hMSC in microtissues

For single transfection, 15 ng chordin siRNA (Dharmacon, Lafayette, Colorado) was complexed with Lipofectamine® RNAiMAX (Thermo Scientific™, Germany) for 5–10 min at RT according to the manufacturer's instructions (for siRNA sequence see Table 1). Complexed siRNA was added to 10^4 cells in 200 μl OptiMEM® with 10% FBS. After 30 min, 100 μl of cGM suspension (6.4 μg•ml^{-1}) in OptiMEM® supplemented with 10% FBS was added and carefully pivoted. Next day, the medium was changed to osteogenic medium by partially removing 200 μl transfection medium and addition of 200 μl fresh medium, twice.

For cGM-based transfection, 703.13 ng Chordin siRNA and 15.78 μl Lipofectamine® RNAiMAX were complexed in 24 μl for 5–10 min at RT, added to 3 mg dried cGM and vortexed immediately for 5 s and incubated at 4 °C for 30 min. Subsequently, loaded cGM were resuspended in 4687.5 μl OptiMEM® supplemented with 10% FBS. 100 μl corresponds with a cGM mass of 0.064 mg loaded with 15 ng siRNA. Then, cell suspension and cGM suspension were mixed in one well of a low adhesion 96 well plate and gently shaken for 1–3 s. Samples were incubated at 37 °C and 5% CO_2. Medium was changed to OM or OM^{+BMP-2} after 24 h. Medium change or washing steps were performed partially twice by careful removing of 200 μl used medium and replacing by 200 μl fresh medium.

In order to exclude off-target effects, All Stars Negative Control siRNA (Qiagen, Hilden, Germany) was used as a non-coding control.

Table 2
TagMan™ Gene Expression assays.

Target		
ALPL	Alkaline phosphatase activity, liver/bone/kidney	HS01029144_m1
CHRD	Chordin	HS00415315_m1
IBSP	Integrin-binding sialo Protein	HS00173720_m1
OCN	Osteocalcin	Hs01587814_g1
RPLP0	60S acidic ribosomal protein P0	HS99999902_m1
RUNX2	Runt-related transcription factor 2	HS00231692_m1

2.9. Co-culturing of differentiated microtissues with hMSC

Microparticles were loaded with siRNA and assembled into microtissues with hMSC as described above. Microtissues were cultured for seven days in OM or OM^{+BMP-2}. A hMSC suspension with 6.0•10^4 cells/well was seeded 24 h prior co-culture in a 24 well plate. Two microtissues/well being added to adherent hMSC monolayer at the well edges. Samples were cultivated in OM without BMP-2 and analyzed after ten days.

2.10. Quantitative RT-PCR

Medium was removed and samples were washed with warm PBS (37 °C). Microtissues were collected in Eppendorf tubes and centrifuged at 420 rcf for 5 min in order to remove remaining PBS. Total RNA was isolated with RNeasy® Mini Kit (Qiagen, Hilden, Germany) including on-column DNA digestion according to the manufacturer's instructions. RNA quantity and purity were determined using Synergy H1 (BioTek, Bad Friedrichshall, Germany) and Take3 Micro-Volume Plate (BioTek, Bad Friedrichshall, Germany). Synthesis of cDNA was performed using High-Capacity cDNA Reverse Transcription Kit (Applied Biosystems™, Thermo Scientific™, Germany) according to the manual. 500–1000 ng of total RNA were reversely transcribed. Real time PCR was performed with BioRad CFX Touch (BioRad, Feldkirchen, Germany) using TaqMan™ Universal Master-Mix for PCR (Applied Biosystems™, Thermo Scientific™, Germany) and TaqMan Gene Expression Assay (Applied Biosystems™, Thermo Scientific™, Germany) in Multiplate® PCR Plates™ (BioRad, Feldkirchen, Germany). The real-time PCR conditions were as follows: at 50 °C for 2 min, polymerase activation at 95 °C for 10 min, followed by 40 cycles of 95 °C for 15 s and 60 °C for 60 s 60S acidic ribosomal protein P0 (RPLP0) is very stable during osteogenic differentiation of hMSC and was used as housekeeping gene [20]. Used TaqMan™ probes are listed in Table 2. Gene expression levels were calculated with reference to non-treated cells and set to 1 as control.

2.11. DNA content

Medium was removed and samples were washed with warm PBS (37 °C). The DNA quantity was measured in a Plate Reader Synergy H1 (BioTek, Bad Friedrichshall, Germany) using Quant-iT™ PicoGreen™ dsDNA (Invitrogen™, Darmstadt, Germany) following a previously described protocol [14,21]. A standard curve of increasing DNA dilutions (Invitrogen™, Darmstadt, Germany) in a range of 0.001–10 μg/ml was used for quantification of unknown samples.

2.12. Alkaline phosphatase (ALP) activity

Medium was removed and samples were washed with warm PBS (37 °C). Cell lysis and measurement of ALP activity were performed following a previously described protocol [14,21] in a Plate Reader Synergy H1 (BioTek, Bad Friedrichshall, Germany). ALP activity was normalized to the DNA content per microtissue determined at the same time points.

2.13. Live-dead-staining

Medium was removed and samples were washed with warm PBS (37

°C). Live-dead-staining was performed following a previously described protocol [22] and analyzed with confocal microscope Leica TCS SP8 and LAS X Software (Leica, Wetzlar, Germany).

2.14. Osteoimage™ mineralization assay

Mineralization was analyzed by staining hydroxyapatite with Osteo-Image (Lonza, Basel, Switzerland). Microtissues were carefully washed

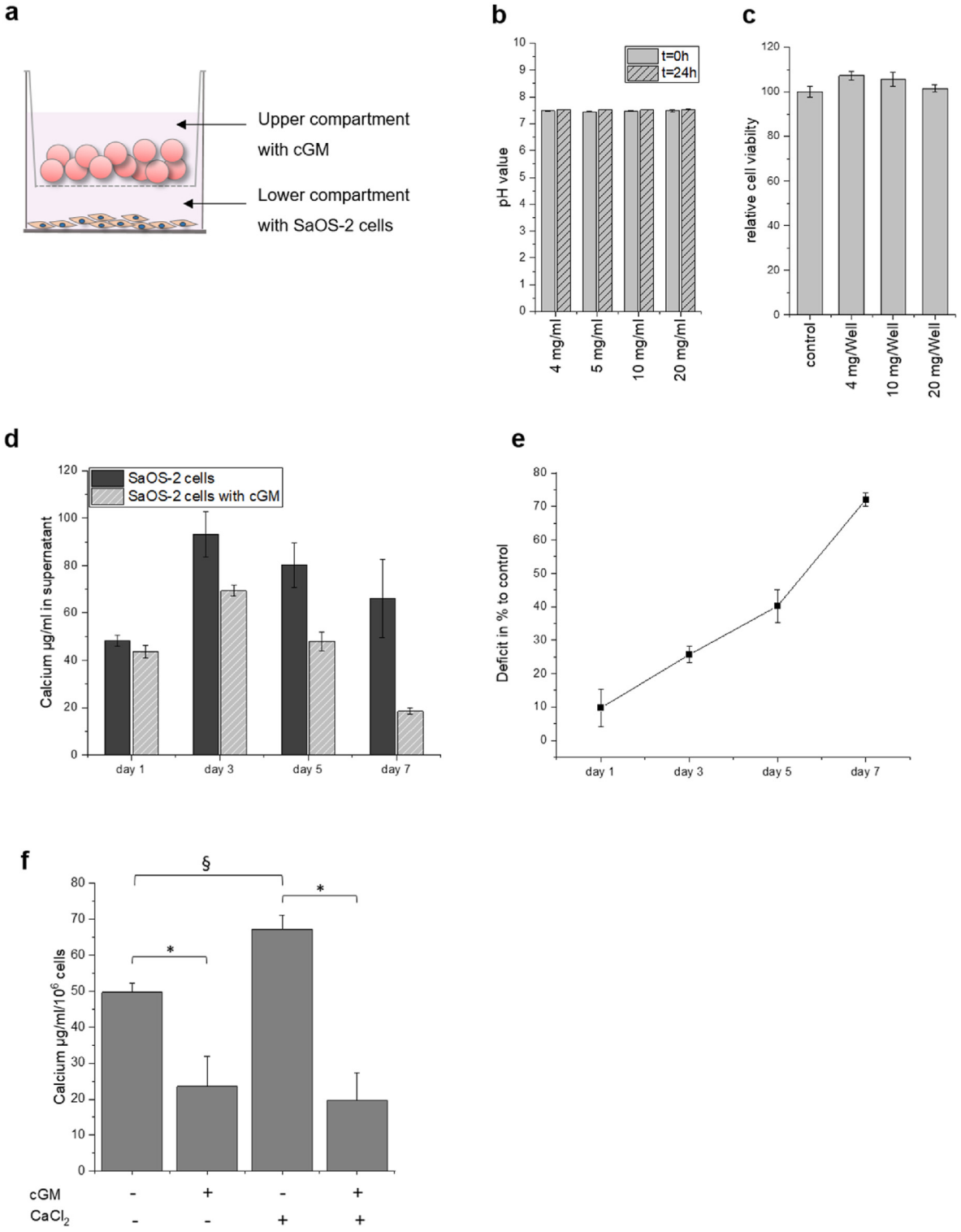

Fig. 2. (a) Schematic illustration of transwell system used for pH measurement, cell viability and calcium ion binding. (b) Stability of pH value of surrounding medium in presence of varying cGM concentrations over 24 h. (c) Cytocompatibility of varying cGM concentrations with SaOS-2 cells after 48 h. Cell viability was normalized to non-treated control without cGM in the upper chamber. (d) Relative calcium ion concentration in the supernatant of SaOS-2 cells cultivated in osteogenic medium for 7 days with and without cGM in the upper chamber of a transwell system. (e) Calcium ion deficit in supernatants in local distance to cGM normalized to samples without cGM. (f) Mineralization of SaOS-2 cells in presence or absence of cGM. Statistically significant differences ($p < 0.05$) are indicated with (*) between with and without cGM and (§) between control group with and without $CaCl_2$ supplementation.

with warm PBS (37 °C) and fixed with 10% paraformaldehyde (PFA) for 1 h at RT. Staining was performed according to manual. For visualizing cell morphology, samples were stained with 1 μl 4′,6-diamidino-2-phenylindole (DAPI) and 25 μl Alexa Fluor™ 568 Phalloidine (Thermo Scientific™, Germany) per 1 ml 2% BSA in PBS for 1 h at RT protected from light. Then, cells were washed twice with 2% BSA in PBS for 5 min each. For imaging confocal microscope Leica TCS SP8 and LAS X Software (Leica, Wetzlar, Germany) were used.

2.15. Alizarin red staining (ARS)

Medium was removed and samples were carefully washed with warm PBS (37 °C). Samples were fixed with 10% PFA for 1 h at RT. After fixation, samples were washed twice with dH_2O. Staining was performed with filtered 40 mM alizarin red S pH 4.2 (1:100 dilution; Sigma Aldrich, adjusted by ammonia hydroxide) for 15 min at RT and gentle shaking. Dye was removed and samples were washed 5 times with dH_2O. Quantification was performed with ImageJ (National Institutes of Health, USA) by binarization and determination of the ARS positive area. Results were normalized to non-treated control.

2.16. Statistics

Statistical testing of mean differences was performed in Microsoft Excel and GraphPad Prism (version 9.2.0) using one-way or two-way analysis of variance (ANOVA) and Tukey post hoc test. Statistically significant differences between groups ($p < 0.05$) are indicated by (*), (§) or (#).

3. Results

3.1. Characterization of oPNMA-7.5+DEED-cross-linked gelatin microparticles

DEED-derivatized cGM were obtained as a free flowing, dry powder with a degree of cross-linking of 37.2% and an average particle size of D [3,4] = 70.8 μm in the dry state (Figure S1). The factor of PBS uptake, which is important for the post-fabricated loading of cGM by swelling,

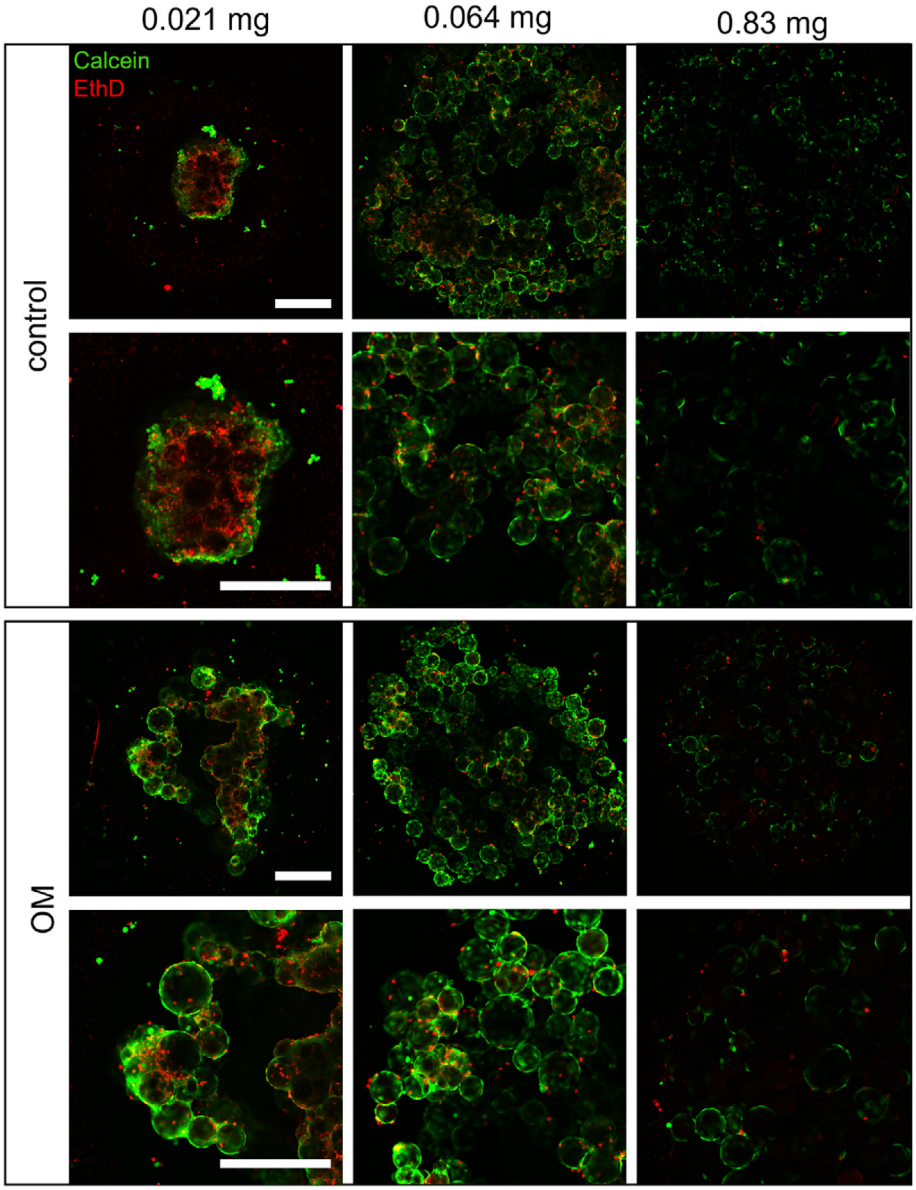

Fig. 3. Live-dead staining of SaOS-2 microtissues after 96 h of cultivation. Representative confocal laser scanning microscopy images (green: Calcein, red: Ethidium homodimer) illustrating the effects of particle amount per microtissue and medium (control: culture medium, OM: osteogenic medium). Scale bar represents 500 μm.

was calculated to be 12.4. The average particle size of the particles swollen in PBS overnight is D [3,4] = 130 μm.

3.2. Stability, cytocompatibility and calcium ion absorption of cGM

In a first approach, we investigated the influence of functional groups of the cross-linker on the pH value of the cell culture medium and cell viability. The separation of particles and cells in the transwell system enabled a focused analysis with exclusion of mechanical stress, hypoxia or physical interactions between cells and material (Fig. 2a). After 24 h in OptiMEM® with 10% FBS we determined no effect on medium pH (Fig. 2b), even in presence of large amounts of cGM. No cytotoxic effects in SaOS-2 cell culture were detectable after incubation for 48 h in the transwell setup with 4, 10 or 20 mg cGM per well (Fig. 2c). Surprisingly, upon osteogenic stimulation of SaOS-2 cells, we determined an increasing depletion of calcium ions from the supernatant medium compared to wells without cGM (Fig. 2d/e) with the consequence of reduced mineral formation in the cell culture (data not shown). The supplementation of calcium ions by the addition of $CaCl_2$ to OM influenced cell mineralization in absence of cGM but not in presence of the particles (Fig. 2f). Gelatin microparticles added to SaOS-2 or hMSC in 2D culture remained stable over the entire cultivation time of up to 40 days. Preliminary *in vitro* tests with collagenase A showed, that the particles are completely enzymatically degradable (data not shown).

3.3. Development of microtissues with different cell types

Having in mind that cGM may accumulate calcium ions, we aimed to establish a protocol to combine cGM and osteogenic cells in microtissues to get a close contact. For the proof-of-concept, SaOS-2 cells were used as model system for osteogenic cells. First, different amounts of cGM, 0.021 mg, 0.064 mg and 0.83 mg, were mixed with a cell suspension with 10^4 cells in a spheroid micro well and incubated with CM or OM for 96 h (Fig. 3). Live-dead-staining was performed, and samples were analyzed with confocal laser scanning microscopy. Microtissues incubated in OM apparently showed more living cells and less densely packed structures in the inner core than in CM. Samples with no or low amounts (0.021 mg) of cGM in CM showed a typical necrotic core (red) and an outer proliferation zone (green), which is known from other pellet cultures [3]. This effect was mitigated by an increased particle fraction per microtissue.

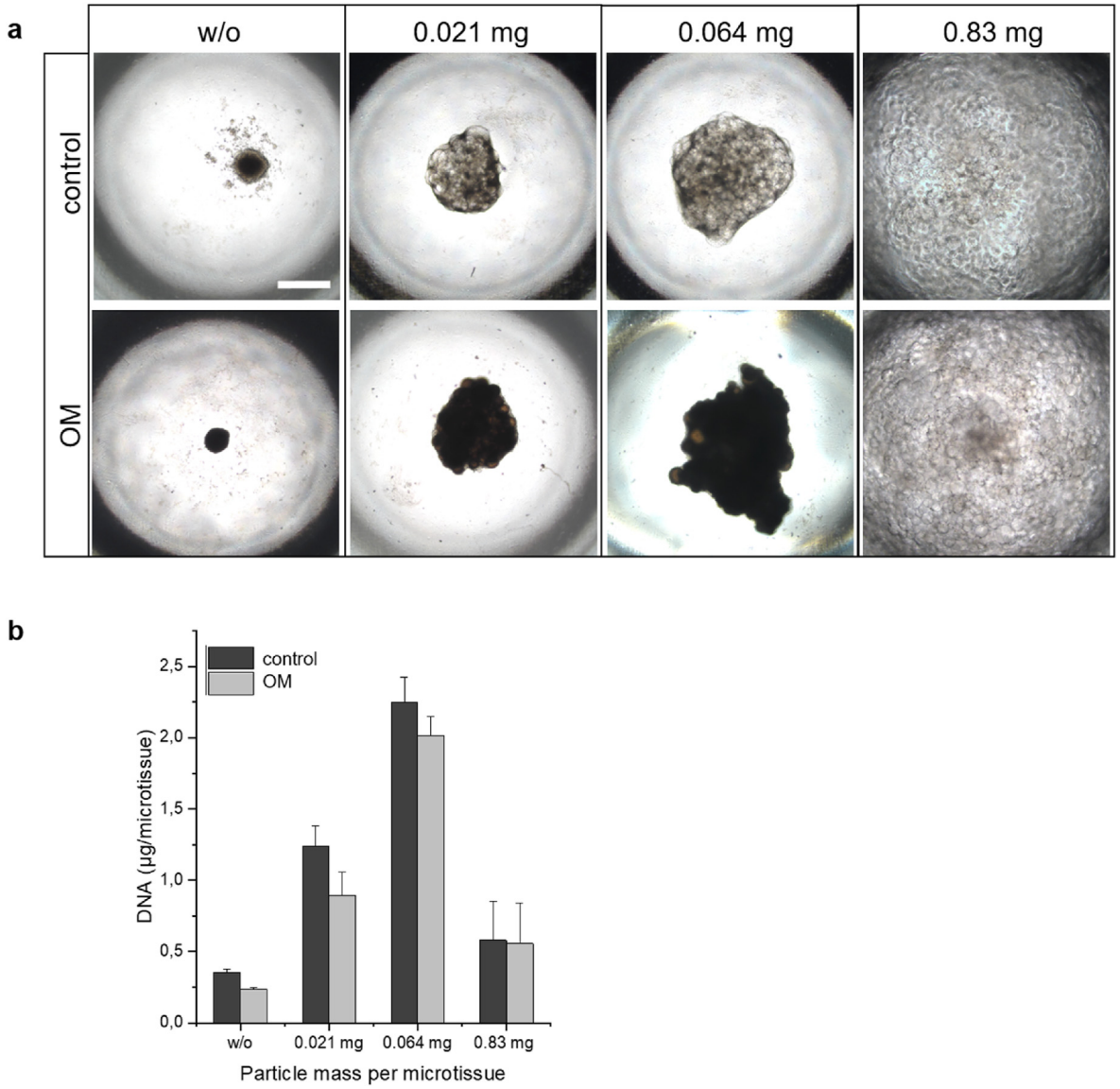

Fig. 4. (a) Effects of particle mass and medium type on morphology and tissue formation of SaOS-2 cell-based microtissues after 7 day of culture. Representative phase contrast images (black and brown shades indicate mineralization) and (b) DNA content of microtissues on day 7. control: culture medium, OM: osteogenic medium. Scale bar represents 500 μm.

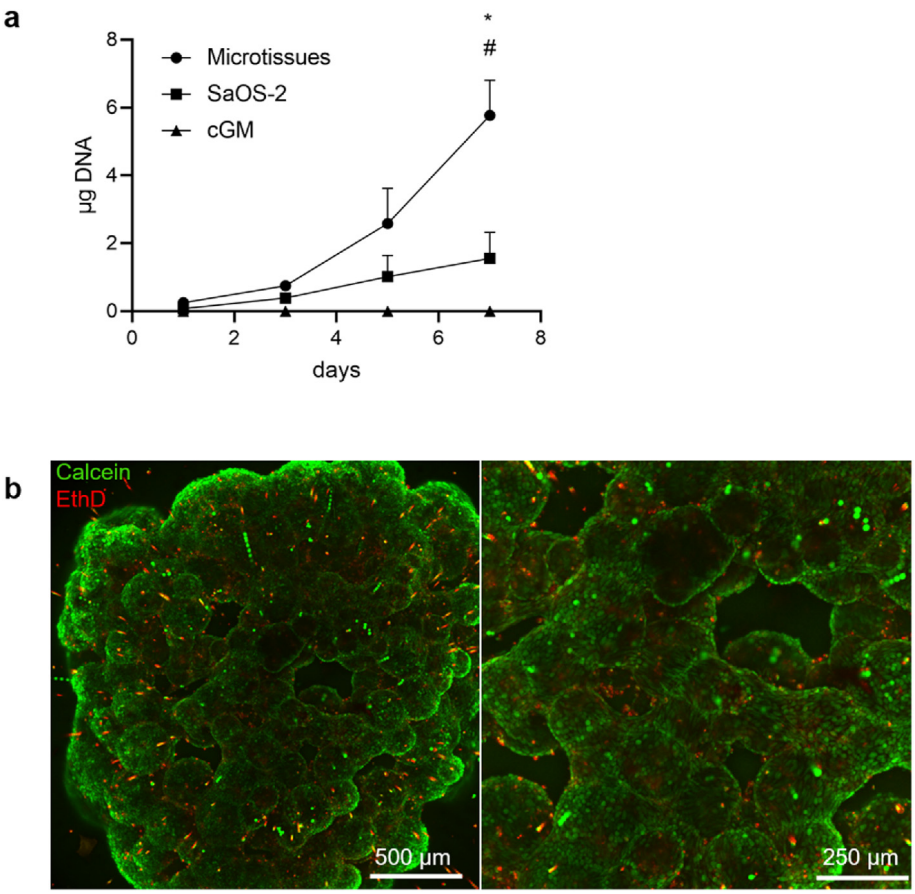

Fig. 5. Biocompatibility of cGM: (a) DNA content as a measure of cell proliferation in microtissues with SaOS-2 cells over 7 days in culture medium. (b) Live-dead-staining of microtissues with SaOS-2 cells after 7 days in osteogenic medium (green: Calcein, red: Ethidium homodimer). Representative confocal laser scanning microscopy images. Statistically significant differences ($p < 0.05$) are indicated with (*) between microtissues and SaOS-2 only and with (#) between microtissues and cGM only.

Mineralization of microtissues was visually estimated by appearance of brown color after 7 days (Fig. 4a). DNA content, as a measure for cell proliferation, showed a maximum with a cGM amount of 0.064 mg/microtissue while lower DNA contents were found with either higher or lower cGM amounts in medium with and without osteogenic supplements (Fig. 4b). Based on the data from the live-dead-staining and the mineralization studies, the optimal cell to particle ratio (10^4 cells/0.064 mg) was used in order to analyze biocompatibility of our material over 7 days in culture medium for SaOS-2 cells (Fig. 5). We measured a continuous increase for DNA and detected completely overgrown microparticles in the live-dead-staining. This cell to particle ratio was then used in the following experiments and transferred to hMSCs.

In order to analyze the quality of deposited minerals, microtissues were stained with OsteoImage™ (green) for hydroxyapatite (Figs. 6 and 7) and analyzed with confocal laser scanning microscopy. Phalloidin staining of cell cytoskeleton revealed a dense network of cells and cGM. On day 7, microtissues from SaOS-2 cells, which were incubated in OM, showed strong mineralization of the incorporated cGM and deposited HA crystals in the matrix around the cells. Cells and particles interact in a dense network, but with less compactness than in CM only. Microtissues from hMSC showed a round and compact structure after 28 days. Mineralization of stem cell-based microtissues occurred after 24–28 days in OM^{+BMP-2} and was focused on the incorporated cGM as seen in SaOS-2 microtissues.

3.4. Chordin silencing & BMP-2 stimulation in microtissues

In the next step, we elaborated the system for the release of siRNA as an active pharmaceutical ingredient (API) (Fig. 8a). As proof-of-concept and positive control, we transfected hMSC with chordin siRNA 30 min before cGM addition. In a second group, hMSC were transfected indirectly by loading the siRNA to cGM. Non-coding siRNA was used to exclude off-target effects. Effective chordin silencing was shown in the directly transfected group after 4 and 6 days, but no significant silencing was found in the cGM-transfected samples (Fig. 8b). Samples in the OM group (without BMP-2) were not significantly influenced by transfection with chordin siRNA in contrast to the BMP-stimulated group. Directly transfected cells as well as indirectly transfected cells showed a significantly increased ALP activity (Fig. 8c). In presence of BMP-2, indirectly transfected microtissues started mineralization already after 14 days and showed higher calcium ion accumulation on day 18 than directly transfected samples (Fig. 8d), whereas mineralization in BMP-2 stimulated samples without siRNA transfection started after 24 days.

In addition to the protein and mineralization data, we analyzed gene expression of osteogenic markers in cGM-transfected microtissues to evaluate the differentiation to the osteogenic lineage (Fig. 9). ALP, IBSP and OCN expression in chordin-silenced samples were significantly increased in comparison to control groups when microtissues were incubated in OM. However, we could not detect differences in microtissues cultivated in OM^{+BMP-2} at the investigated time points except for OCN in the early phase.

3.5. Induction of mineralization in undifferentiated hMSC

To investigate possible paracrine osteogenic effects of differentiated microtissues on undifferentiated hMSC, we incubated freshly seeded hMSC with differentiated microtissues in OM for further 10 days. For microtissue formation, cGM were loaded with siRNA and incorporated into hMSC aggregates. Microtissues were differentiated for 7 days in OM or OM^{+BMP-2} before being added to an adherent hMSC monolayer. Monolayer cells were cultivated in OM without BMP-2 and analyzed on day 10. Microtissues, loaded with chordin siRNA and differentiated with

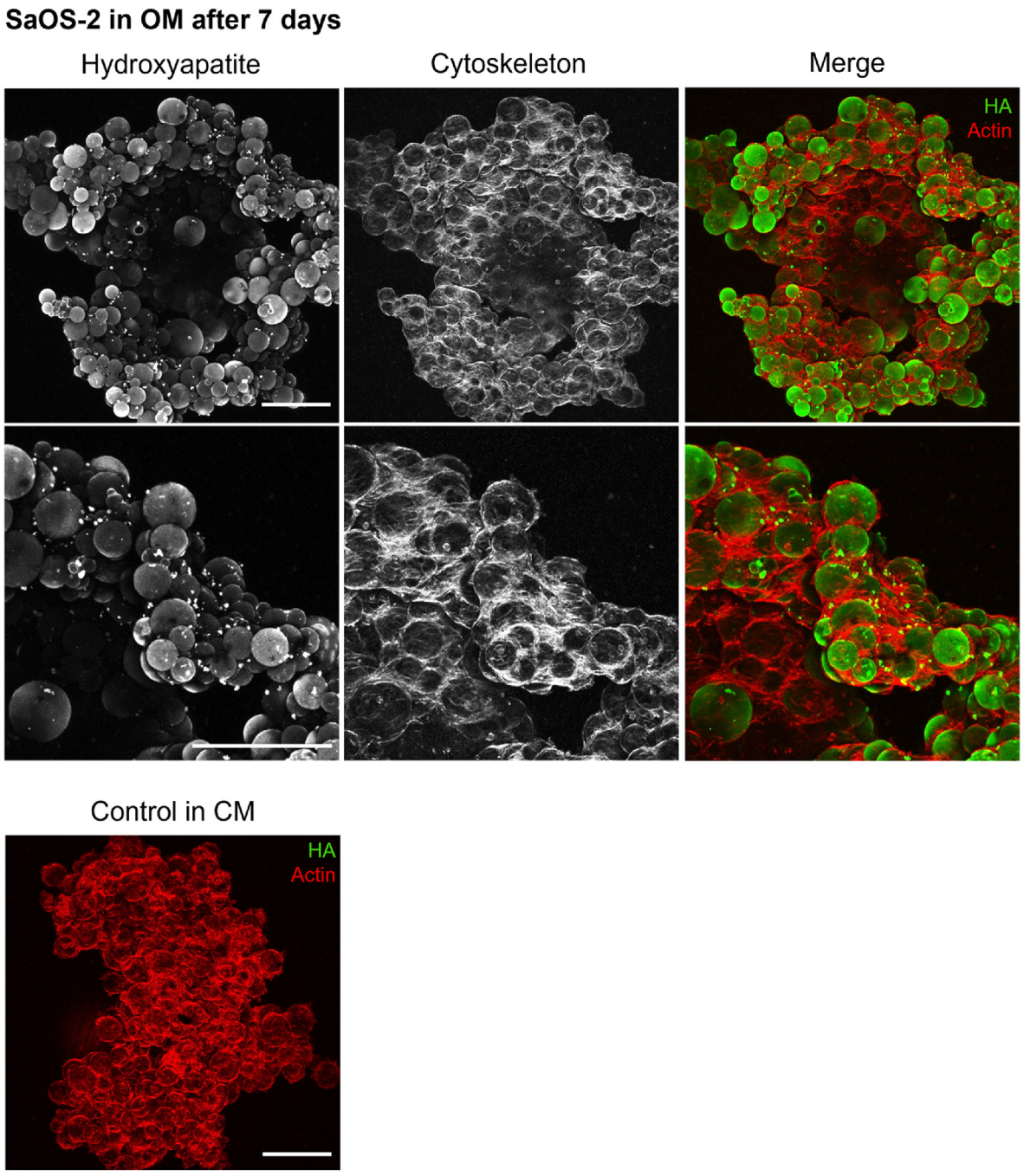

Fig. 6. Mineral formation in SaOS-2 microtissues after 7 days in osteogenic medium (OM). Representative confocal laser scanning microscopy images of Osteoimage® stained hydroxyapatite in microtissues (green: hydroxyapatite, red: actin cytoskeleton). Scale bars represent 500 μm.

BMP-2, started mineralization after 7 days in co-culture with undifferentiated hMSC. After 10 days, mineralization had spread starting from the microtissues, and cells all over the well began to form mineralized matrix (Fig. 10).

4. Discussion

4.1. Mineralized microtissues in an osteogenic environment

The regeneration of defects in tissues by a microparticle-based cell carrier offers several advantages compared to scaffold-based approaches. These include the use of pre-differentiated cells for therapeutic application in combination with a minimally invasive clinical procedure. Additionally, the use of individual single units provides the basis for a modular principle and the construction of multi-unit systems with freely selectable and combinable biophysical (porosity, stiffness, topography, size shape) and biochemical (e.g., antibodies, peptides, carbohydrates, growth factors) properties [23].

Cell-cell interactions take place in all directions in the 3D microtissues and the shape, stiffness and geometry of the microparticle substrate are critical conditions for the cell fate and functional behavior [24]. The generation of tissue-like structures or organoids is gaining attention for

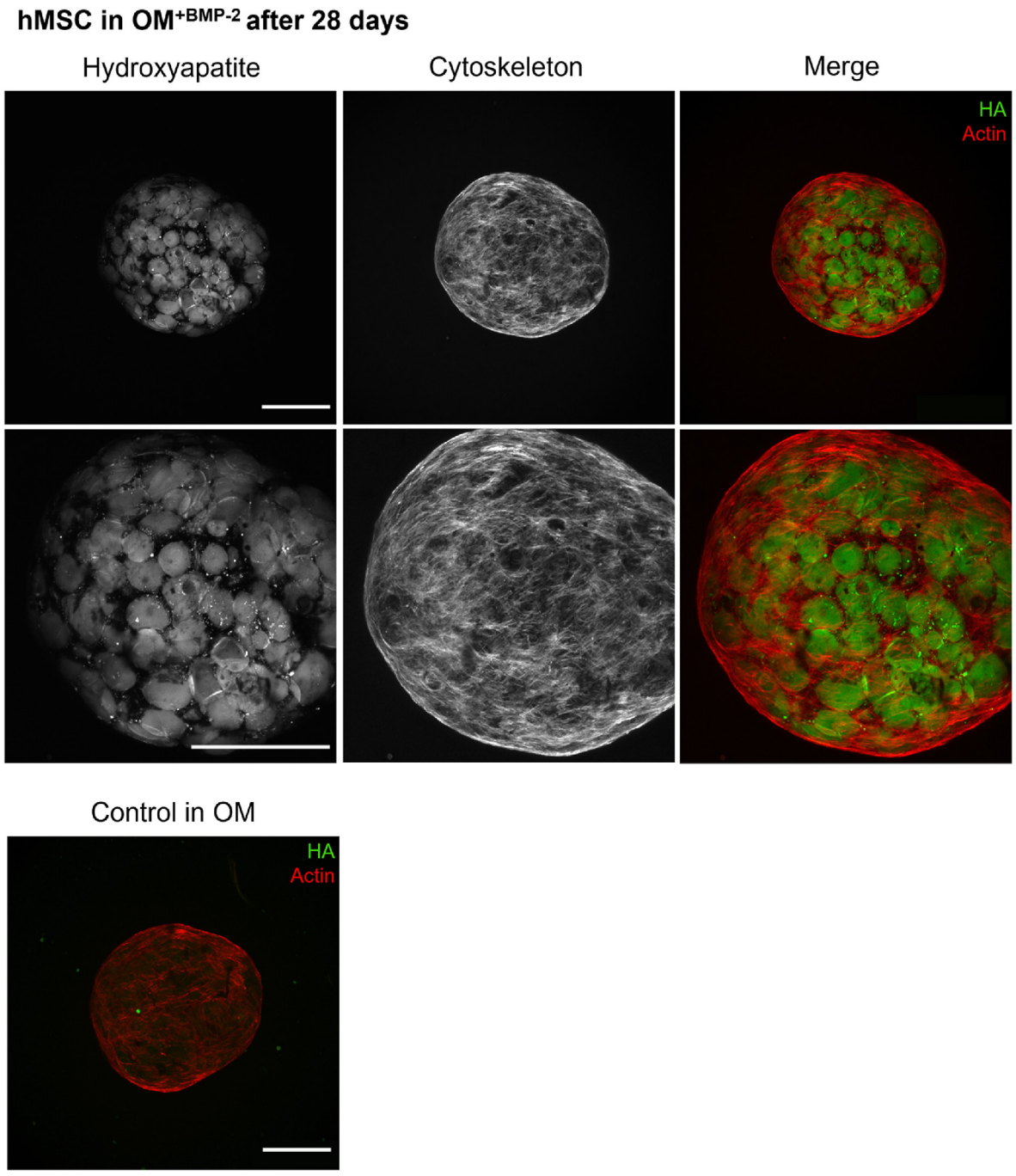

Fig. 7. Mineral formation in hMSC microtissues after 28 days in osteogenic medium (OM $^{+\,BMP-2}$ or control OM). Representative confocal laser scanning microscopy images of Osteoimage® stained hydroxyapatite in microtissues (green: hydroxyapatite, red: actin cytoskeleton). Scale bars represent 500 μm.

regenerative aspects as well as the development of 3D drug screening model systems for a wide range of applications [25]. A common limitation of cell-aggregates is associated with the lack of vascularization and corresponding insufficient transport and diffusion of nutrients or oxygen [4].

In this study, we could demonstrate in different culture media that cell aggregates with cGM show improved proliferation and finally differentiation inside the microtissues. *Tajima* and *Tabata* have published similar effects of the incorporation of gelatin microparticles into cell aggregates in their studies [26,27]. Microtissues were not formed when the amount of cGM was extremely high. This could be explained by the physical suppression of cell-cell-interactions, which is mandatory for cell regulation processes and differentiation [28]. The homogenous distribution of cGM in the microtissues may keep the oxygen level at an acceptable level and support osteogenic differentiation. In dense cell aggregates without or with low amounts of cGM, oxygen level become very low, which may promote stem cell differentiation into chondrocytes [29,30], but may also cause cell death [4]. In order to generate stable microtissues, a balance should be maintained between the degree of cGM incorporation to improve the nutritional properties within the aggregates and the optimal cell density for cell-cell interactions.

Cross-linked gelatin microparticles with DEED-derivatized oPNMA are considered to support calcium ion absorption and mineralization of the microtissues. The existing carboxyl groups in the gelatin and the carboxyl groups built into by the cross-linker increase the negative charges and support calcium ion absorption. Presumably, this also

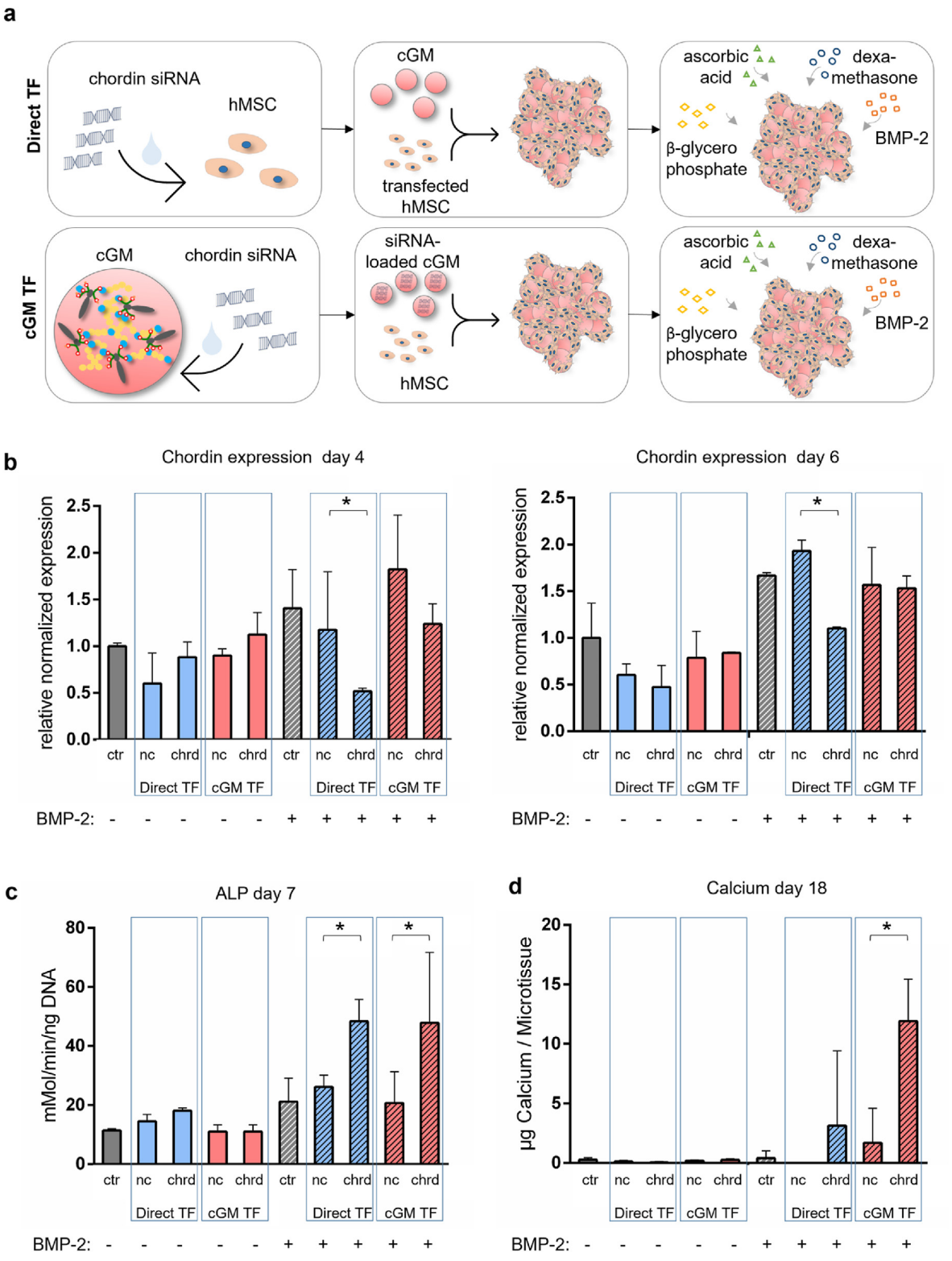

Fig. 8. (a) Experimental set up of microtissues with hMSC and chordin silencing with direct and indirect transfection in OM and OM^{+BMP-2}. (b) Quantification (qPCR) of Chordin expression after 4 and 6 days, (c) ALP activity after 7 days and (d) mineralization after 18 days (ctr: non-treated control, nc: non-coding siRNA, chrd: chordin siRNA). Direct TF: cells transfected 30 min before microtissue assembly, cGM TF: transfection via siRNA-loaded cGM. Statistically significant differences are indicated with (*) between non-coding control and chordin siRNA-treated samples ($p < 0.05$).

increases the nucleation of calcium phosphates and the mineralization ability of cGM. Upon derivatization with DEED, anhydrides were partially aminolyzed and tertiary amine groups were implemented, which reduced the degree of cross-linking and negative charge density [31]. DEED derivatization may alleviate calcium ion binding and promote moderate calcification, which leads to the formation of hydroxyapatite triggered by cells and not from the material alone. A self-mineralization in absence of cells could not be observed within the

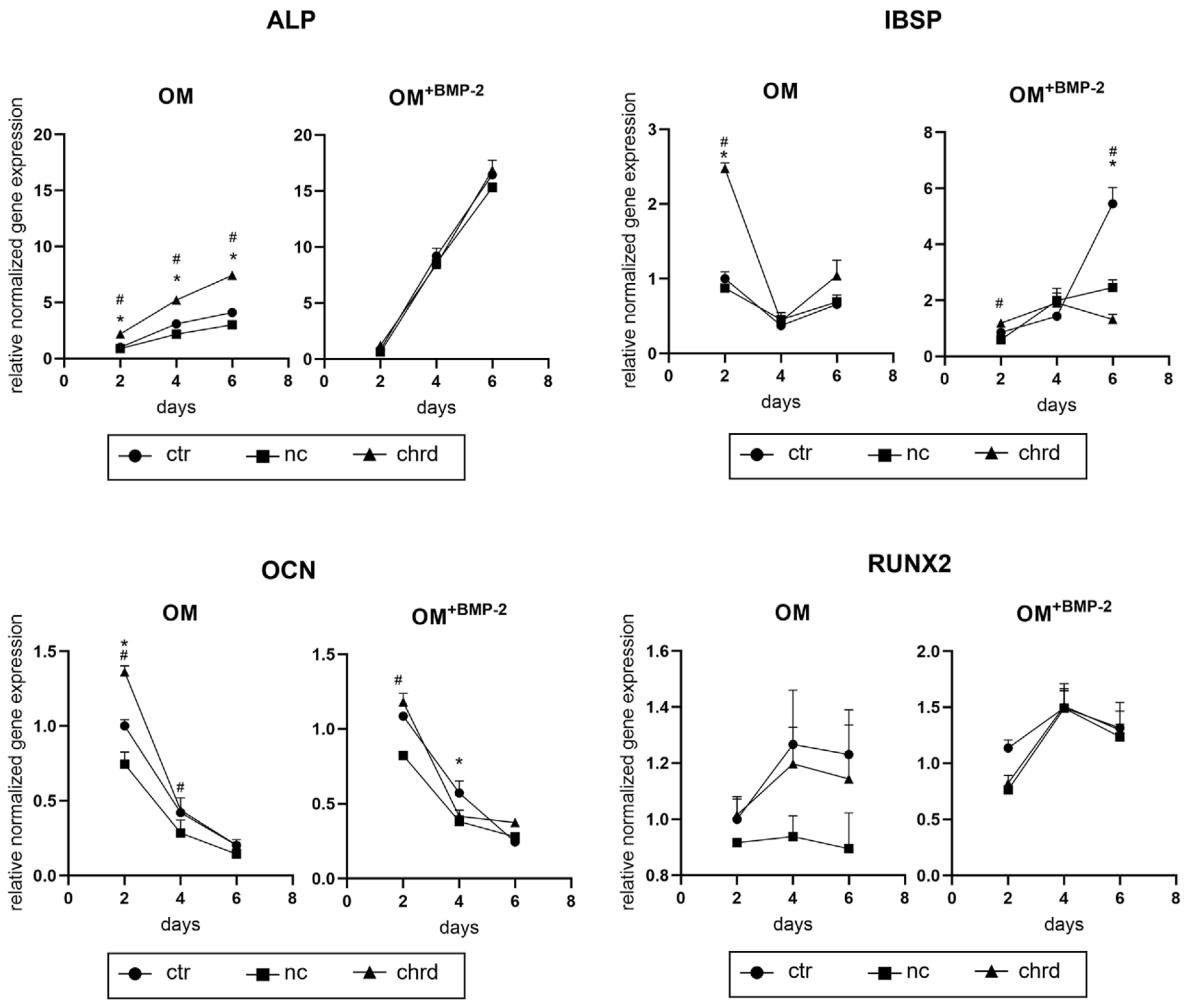

Fig. 9. Effect of chordin silencing effects on relative gene expression of osteogenic markers proteins during early osteogenic differentiation of hMSCs in microtissues. hMSCs were indirectly transfected via cGM. Alkaline phosphatase (ALP), integrin-binding sialo protein (IBSP), osteocalcin (OCN) and runt-related transcription factor 2 (RUNX2) in hMSC microtissues cultivated for 2, 4 and 6 days in OM and OM^{+BMP-2} (ctr: non-treated control, nc: non-coding siRNA, chrd: chordin siRNA). Differences in gene expression were determined using a two-way ANOVA, followed by Tukey's multiple comparisons test. Statistically significant differences are indicated with (*) between non-treated control and chordin siRNA-treated samples and with (#) between non-coding control and chordin siRNA-treated samples ($p < 0.05$).

first 14 days in a calcium- and phosphate-rich medium for the chosen microparticles.

We used an osteogenic medium to supply the cells with β-glycerophosphate as phosphate source and ascorbic acid during osteogenic differentiation. The type of phosphate source could influence the quality of mineralization and act as an intracellular signaling molecule for gene expression of several osteogenic markers [32–35]. Furthermore, we relied on dexamethasone as a standard supplement for osteogenic differentiation [36]. Future studies need to show if osteogenic differentiation in the microtissues will also take place in absence of dexamethasone. As other studies have already shown, the key to osteogenic differentiation may only be in the interaction of the cells with the extracellular matrix [37].

Several non-collagenous proteins can initiate mineralization and regulate the growth of minerals [38–40]. Anionic glutamic acid-rich bone sialoprotein, for example, has been described as important factor for the nucleation of hydroxyapatite. Moreover, osteocalcin, could act as a nucleator for hydroxyapatite when immobilized, but in solution it inhibits mineralization [41,42]. Furthermore, the local pH value plays an important role during hydroxyapatite growth [43]. We assume that the mineralization in our microtissues is a cross-linker and protein-dependent mechanism that needs to be analyzed in more detail in further studies.

Contrary to the claims that BMP-2 is limited to a penetration depth of 200–400 μm thickness [44], we were able to clearly detect an influence of BMP-2 on the cells in the microtissues. This could be explained by the loose structures of cells and particles upon spheroid formation in the first days until compact and stable microtissues are formed. It is known from literature, that a single stimulation with BMP-2 for 15 min induces osteogenic differentiation in hASC [45]. A combination of the biomaterial, calcium ion absorption, serum proteins and osteogenic supplements could be decisive for the osteogenic differentiation under BMP-2. The role of cGM-BMP-2 interaction and possible presentation of protein structures to adherent cells is still unclear and needs to be investigated.

4.2. *Chordin silencing enhances osteogenic differentiation in microtissues*

The cGM can act as delivery devices within the microtissue aggregates, presenting soluble signaling factors or loaded drugs [26,46] besides providing the structural support for cell growth [5,47,48]. Chordin, a naturally occurring and BMP-2-dependent protein, which inhibits the interaction between BMP-2 and BMP-2 receptor, is a promising candidate for bone regeneration [49,50]. Several studies demonstrated an improved osteogenic differentiation by suppression of chordin and simultaneous stimulation with BMP-2 [13–16].

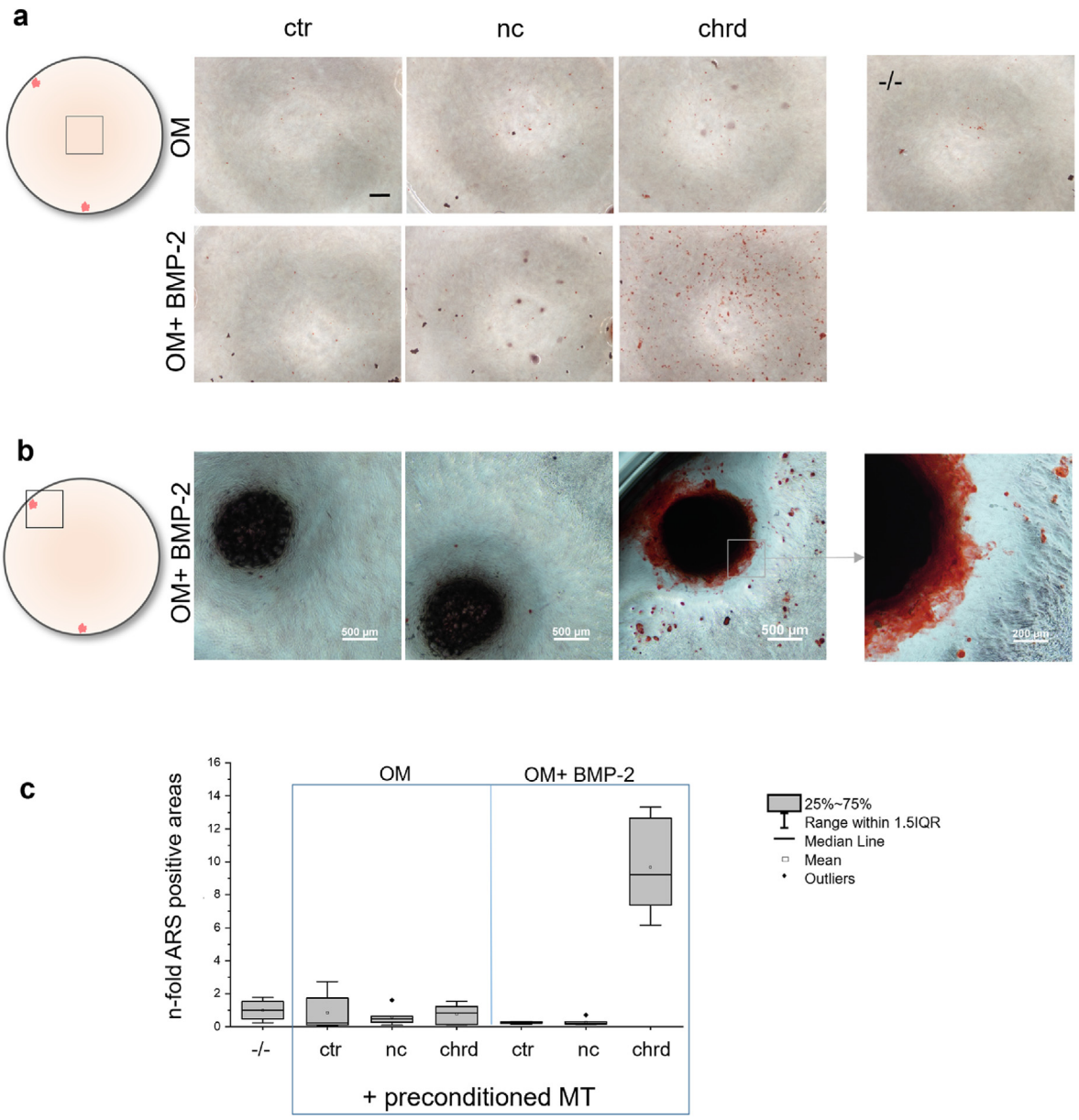

Fig. 10. Induction of mineralization in hMSC monolayer cultured in presence of pre-differentiated microtissues in OM for 10 days (ctr: control, chrd: chordin siRNA, nc: non-coding siRNA). Microtissues formed of hMSC and siRNA-loaded cGM were pre-differentiated in OM^{+BMP-2} for 7 days prior addition to hMSC monolayers. (a) Representative images of hMSC monolayer after Alizarin Red staining in the middle of one well after 10 days of co-culturing. Scale bar: 1000 µm. (b) Microscopic images of Alizarin Red staining (ARS) of the mineralized microtissue after preconditioning with chordin siRNA and BMP-2 stimulation and (c) quantitative analyses of ARS and normalization of samples with different pre-differentiated microtissues to hMSC monolayer alone. Boxplots displaying the measured n-fold ARS positive areas (median and mean values, interquartile range 25–75%).

In our study, we compared direct transfection of hMSC with indirect transfection via siRNA-loaded cGM. In the direct transfection group, stem cells were treated with one dose of chordin siRNA before combining cells and cGM in the spheroid micro wells. In the indirect transfection group, chordin siRNA was loaded to cGM to obtain a local delivery reservoir of siRNA before incorporation in microtissues. In presence of BMP-2 we found in both chordin silenced groups elevated ALP levels compared to non-treated and non-coding control. Samples, initially transfected with chordin siRNA, started mineralization after 18 days. However, samples which were indirectly transfected by cGM-released siRNA showed significantly higher calcium ion deposition compared to the other groups. Despite this convincingly increased ALP and calcium ion deposition, we could only determine a tendency to decreased chordin expression in indirectly transfected microtissues in contrast to the directly transfected group. An explanation for this phenomenon could be a slow but long lasting uptake of siRNA by the cells, which may have initiated osteogenic downstream effects. This implicates that siRNA complexes remain biologically active and are apparently not negatively affected by the particle loading step. We assume, that siRNA complexes interact electrostatically with cGM surface [51] and the majority of the complexes remain in place due to limited diffusional exchange and longer diffusion distances in the aggregate culture. Zeta potential analysis of complexed siRNA (Figure S2) revealed positive surface charges which support loading to cGM and enable binding to negative charged carboxyl groups. In close contact with the microtissue forming cells, cGM immobilized siRNA seems to become available for the cells. Analysis of osteogenic marker gene expression showed differences in the OM groups for ALP, IBSP and OCN. Nonetheless, the OM^{+BMP-2} group showed no clear differences in gene expression, except for OCN in the very early phase of differentiation. We suspect moderate long lasting silencing effects that need to be

investigated more closely in future studies. In summary, we could demonstrate that chordin siRNA delivery by cGM stimulates osteogenic differentiation in microtissues at early points when BMP-2 was supplemented resulting in an increased deposition of mineral at later time points.

4.3. Proof-of-concept: induction of mineralization in 2D hMSC

It has been shown that the use of pre-differentiated MSC is more efficient in bone regeneration than undifferentiated or fully differentiated stem cells [52,53]. In addition, it has been described that mineralized hydrogels are able to induce bone regeneration *in vivo* [12]. In order to set up a simple model to investigate paracrine effects of microtissues, we combined the microtissue approach with undifferentiated conventionally 2D cultured hMSC in a co-culture. Microtissues were loaded with chordin siRNA and stimulated with OM^{+BMP-2} for 7 days prior adding to a non-stimulated hMSC monolayer and co-culturing in OM for further 10 days. We observed that the accelerated differentiation of the microtissues, that took place only after BMP-2 stimulation and cGM-induced chordin silencing, also affected the stem cells that were still undifferentiated in the co-culture. Our data clearly show that the mineralization of the cells in the middle of the well with a large distance from the micro-tissue was also accelerated compared to the control. A control experiment (data not shown) in a transwell system with separated microtissues and hMSC monolayers indicated that the hMSC monolayer was stimulated via paracrine signaling. This supports paracrine osteogenic effects [54] of the microtissues that were missing in cGM loaded with non-coding or without siRNA. Our developed microtissues can induce mineralization presumably directly through cell-cell-contacts and indirectly through secreted soluble factors, which needs to be investigated more closely. By this proof-of-concept experiment, we demonstrated that the treatment with pre-differentiated microtissues may be promising for clinical application.

5. Conclusion

Cross-linked gelatin microparticles were successfully formed assembled with SaOS-2 or hMSC into microtissues. Combined with autologous hMSC, microtissues could be an innovative alternative to autologous transplants used directly for bone tissue engineering via mini open surgery or embedded in a carrier matrix (hydrogel, calcium phosphate cement, fiber mesh, scaffold). In addition, microtissues could provide an interesting system to set up organoid cultures as API test system.

Transfection with siRNA against chordin in addition with continuous BMP-2 treatment leads to an accelerated osteogenic differentiation of hMSC in cGM-based microtissues. In a co-culture model of predifferentiated hMSC microtissues involving cGM mediated chordin silencing with undifferentiated hMSC, we found accelerated osteogenic differentiation of undifferentiated hMSC. This may be considered as an indication for promising *in vivo* osteogenic effects of our microtissues.

Credit author statement

Sandra Hinkelmann: Investigation and writing. Alexandra H. Springwald: investigation and writing. Annett Starke: resources and investigation. Hermann Kalwa: CLSM methodology and CLSM supervision. Christian Wölk: Conceptualization. Michael C. Hacker: Conceptualization, Writing – review & editing, Formal analysis, Supervision. Michaela Schulz-Siegmund: Conceptualization, Supervision, Writing – review & editing, Funding acquisition.

Data availability

The raw/processed data required to reproduce these findings cannot be shared at this time due to technical or time limitations.

Declaration of competing interest

The authors declare that they have no known competing financial interests or personal relationships that could have appeared to influence the work reported in this paper.

Acknowledgements

We thank for financial support by the Deutsche Forschungsgemeinschaft (DFG, German Research Foundation) - Projektnummer 59307082 - TRR67 (subproject A1) and the Sächsische Aufbaubank (SAB)/Saxonian Ministry of Science and Art (SMWK), grant number 100242662.

Appendix A. Supplementary data

Supplementary data to this article can be found online at https://doi.org/10.1016/j.mtbio.2021.100190.

References

[1] A. Busch, A. Wegner, M. Haversath, M. Jäger, Knochenersatzmaterialien in der orthopädischen Chirurgie: von der aktuellen Situation zu künftigen Entwicklungen, Zeitschrift fur Orthopadie und Unfallchirurgie, 2020, https://doi.org/10.1055/a-1073-8473.
[2] J. Ng, K. Spiller, J. Bernhard, G. Vunjak-Novakovic, Biomimetic approaches for bone tissue engineering, Tissue engineering, part B, reviews 23 (2017) 480–493, https://doi.org/10.1089/ten.TEB.2016.0289.
[3] R.-Z. Lin, R.-Z. Lin, H.-Y. Chang, Recent advances in three-dimensional multicellular spheroid culture for biomedical research, Biotechnol. J. 3 (2008) 1172–1184, https://doi.org/10.1002/biot.200700228.
[4] K. Kellner, G. Liebsch, I. Klimant, O.S. Wolfbeis, T. Blunk, M.B. Schulz, A. Göpferich, Determination of oxygen gradients in engineered tissue using a fluorescent sensor, Biotechnol. Bioeng. 80 (2002) 73–83, https://doi.org/10.1002/bit.10352.
[5] K. Hayashi, Y. Tabata, Preparation of stem cell aggregates with gelatin microspheres to enhance biological functions, Acta Biomater. 7 (2011) 2797–2803, https://doi.org/10.1016/j.actbio.2011.04.013.
[6] L.P. Ferreira, V.M. Gaspar, J.F. Mano, Bioinstructive microparticles for self-assembly of mesenchymal stem cell-3D tumor spheroids, Biomaterials 185 (2018) 155–173, https://doi.org/10.1016/j.biomaterials.2018.09.007.
[7] T. Loth, R. Hötzel, C. Kascholke, U. Anderegg, M. Schulz-Siegmund, M.C. Hacker, Gelatin-based biomaterial engineering with anhydride-containing oligomeric cross-linkers, Biomacromolecules 15 (2014) 2104–2118, https://doi.org/10.1021/bm500241y.
[8] C. Kohn, J.M. Klemens, C. Kascholke, N.S. Murthy, J. Kohn, M. Brandenburger, M.C. Hacker, Dual-component collagenous peptide/reactive oligomer hydrogels as potential nerve guidance materials - from characterization to functionalization, Biomat. Sci. 4 (2016) 1605–1621, https://doi.org/10.1039/c6bm00397d.
[9] T. Loth, R. Hennig, C. Kascholke, R. Hötzel, M.C. Hacker, Reactive and stimuli-responsive maleic anhydride containing macromers – multi-functional cross-linkers and building blocks for hydrogel fabrication, React. Funct. Polym. 73 (2013) 1480–1492, https://doi.org/10.1016/j.reactfunctpolym.2013.08.002.
[10] H. Kang, Y.-R.V. Shih, Y. Hwang, C. Wen, V. Rao, T. Seo, S. Varghese, Mineralized gelatin methacrylate-based matrices induce osteogenic differentiation of human induced pluripotent stem cells, Acta Biomater. 10 (2014) 4961–4970, https://doi.org/10.1016/j.actbio.2014.08.010.
[11] C. Heinemann, S. Heinemann, S. Rößler, B. Kruppke, H.-P. Wiesmann, T. Hanke, Organically modified hydroxyapatite (ormoHAP) nanospheres stimulate the differentiation of osteoblast and osteoclast precursors: a co-culture study, Biomed. Mater. 14 (2019) 35015, https://doi.org/10.1088/1748-605X/ab0fad.
[12] X. Wu, T. Zhang, B. Hoff, S. Suvarnapathaki, D. Lantigua, C. McCarthy, B. Wu, G. Camci-Unal, Mineralized hydrogels induce bone regeneration in critical size cranial defects, Adv. Healthcare Mat. 10 (2021), e2001101, https://doi.org/10.1002/adhm.202001101.
[13] C. Wang, F. Xiao, Y. Gan, W. Yuan, Z. Zhai, T. Jin, X. Chen, X. Zhang, Improving bone regeneration using chordin siRNA delivered by pH-responsive and non-toxic polyspermine imidazole-4,5-Imine, Cellular physiology and biochemistry, Int. J. Exp. Cellular Physio. Biochem. Pharmacol. 46 (2018) 133–147, https://doi.org/10.1159/000488416.
[14] H. Schneider, B. Sedaghati, A. Naumann, M.C. Hacker, M. Schulz-Siegmund, Gene silencing of chordin improves BMP-2 effects on osteogenic differentiation of human adipose tissue-derived stromal cells, Tissue engineering, part A 20 (2014) 335–345, https://doi.org/10.1089/ten.tea.2012.0563.
[15] F.N.K. Kwong, S.M. Richardson, C.H. Evans, Chordin knockdown enhances the osteogenic differentiation of human mesenchymal stem cells, Arthritis Res. Ther. 10 (2008) R65, https://doi.org/10.1186/ar2436.
[16] C. Wang, W. Yuan, F. Xiao, Y. Gan, X. Zhao, Z. Zhai, X. Zhao, C. Zhao, P. Cui, T. Jin, X. Chen, X. Zhang, Biscarbamate cross-linked low-molecular-weight polyethylenimine for delivering anti-chordin siRNA into human mesenchymal stem

cells for improving bone regeneration, Front. Pharmacol. 8 (2017) 572, https://doi.org/10.3389/fphar.2017.00572.
[17] W.A. Bubnis, C.M. Ofner, The determination of ε-amino groups in soluble and poorly soluble proteinaceous materials by a spectrophotometrie method using trinitrobenzenesulfonic acid, Anal. Biochem. 207 (1992) 129–133, https://doi.org/10.1016/0003-2697(92)90513-7.
[18] T.A. Holland, Y. Tabata, A.G. Mikos, In vitro release of transforming growth factor-β1 from gelatin microparticles encapsulated in biodegradable, injectable oligo(poly(ethylene glycol) fumarate) hydrogels, J. Contr. Release 91 (2003) 299–313, https://doi.org/10.1016/S0168-3659(03)00258-X.
[19] A. Bertolo, A. Gemperli, M. Gruber, B. Gantenbein, M. Baur, T. Pötzel, J. Stoyanov, In vitro cell motility as a potential mesenchymal stem cell marker for multipotency, Stem Cells Trans. Med. 4 (2015) 84–90, https://doi.org/10.5966/sctm.2014-0156.
[20] A. Jacobi, J. Rauh, P. Bernstein, C. Liebers, X. Zou, M. Stiehler, Comparative analysis of reference gene stability in human mesenchymal stromal cells during osteogenic differentiation, Biotechnol. Prog. 29 (2013) 1034–1042, https://doi.org/10.1002/btpr.1747.
[21] B. Sedaghati, R. Jahroomishirazi, A. Starke, M.C. Hacker, M. Schulz-Siegmund, Rat osteosarcoma cells as a therapeutic target model for osteoregeneration via sclerostin knockdown, Cells, tissues, organs 201 (2016) 366–379, https://doi.org/10.1159/000444634.
[22] H.A. Nawaz, K. Schröck, M. Schmid, J. Krieghoff, I. Maqsood, C. Kascholke, C. Kohn-Polster, M. Schulz-Siegmund, M.C. Hacker, Injectable oligomer-cross-linked gelatine hydrogels via anhydride-amine-conjugation, J. Mater. Chem. B 9 (2021) 2295–2307, https://doi.org/10.1039/D0TB02861D.
[23] M.D. Neto, M.B. Oliveira, J.F. Mano, Microparticles in contact with cells: from carriers to multifunctional tissue modulators, Trends Biotechnol. 37 (2019) 1011–1028, https://doi.org/10.1016/j.tibtech.2019.02.008.
[24] F. D'Angelo, R. Tiribuzi, I. Armentano, J.M. Kenny, S. Martino, A. Orlacchio, Mechanotransduction: tuning stem cells fate, J. Funct. Biomater. 2 (2011) 67–87, https://doi.org/10.3390/jfb2020067.
[25] M. Hofer, M.P. Lutolf, Engineering organoids, Nat. Rev. Mater. 6 (2021) 1–19, https://doi.org/10.1038/s41578-021-00279-y.
[26] S. Tajima, Y. Tabata, Preparation of cell aggregates incorporating gelatin hydrogel microspheres containing bone morphogenic protein-2 with different degradabilities, Journal of biomaterials science, Polymer edition 29 (2018) 775–792, https://doi.org/10.1080/09205063.2017.1358547.
[27] S. Tajima, Y. Tabata, Preparation and functional evaluation of cell aggregates incorporating gelatin microspheres with different degradabilities, J. Tissue Eng. Regenerative Med. 7 (2013) 801–811, https://doi.org/10.1002/term.1469.
[28] J. Tang, R. Peng, J. Ding, The regulation of stem cell differentiation by cell-cell contact on micropatterned material surfaces, Biomaterials 31 (2010) 2470–2476, https://doi.org/10.1016/j.biomaterials.2009.12.006.
[29] M. Kanichai, D. Ferguson, P.J. Prendergast, V.A. Campbell, Hypoxia promotes chondrogenesis in rat mesenchymal stem cells: a role for AKT and hypoxia-inducible factor (HIF)-1alpha, J. Cell. Physiol. 216 (2008) 708–715, https://doi.org/10.1002/jcp.21446.
[30] D.P. Lennon, J.M. Edmison, A.I. Caplan, Cultivation of rat marrow-derived mesenchymal stem cells in reduced oxygen tension: effects on in vitro and in vivo osteochondrogenesis, J. Cell. Physiol. 187 (2001) 345–355, https://doi.org/10.1002/jcp.1081.
[31] L. Zhou, G. Tan, Y. Tan, H. Wang, J. Liao, C. Ning, Biomimetic mineralization of anionic gelatin hydrogels: effect of degree of methacrylation, RSC Adv. 4 (2014) 21997–22008, https://doi.org/10.1039/c4ra02271h.
[32] L.M. Schäck, S. Noack, R. Winkler, G. Wißmann, P. Behrens, M. Wellmann, M. Jagodzinski, C. Krettek, A. Hoffmann, The phosphate source influences gene expression and quality of mineralization during in vitro osteogenic differentiation of human mesenchymal stem cells, PLoS One 8 (2013), e65943, https://doi.org/10.1371/journal.pone.0065943.
[33] B.L. Foster, F.H. Nociti, E.C. Swanson, D. Matsa-Dunn, J.E. Berry, C.J. Cupp, P. Zhang, M.J. Somerman, Regulation of cementoblast gene expression by inorganic phosphate in vitro, Calcif. Tissue Int. 78 (2006) 103–112, https://doi.org/10.1007/s00223-005-0184-7.
[34] S. Fatherazi, D. Matsa-Dunn, B.L. Foster, R.B. Rutherford, M.J. Somerman, R.B. Presland, Phosphate regulates osteopontin gene transcription, J. Dent. Res. 88 (2009) 39–44, https://doi.org/10.1177/0022034508328072.
[35] H. Tada, E. Nemoto, B.L. Foster, M.J. Somerman, H. Shimauchi, Phosphate increases bone morphogenetic protein-2 expression through cAMP-dependent protein kinase and ERK1/2 pathways in human dental pulp cells, Bone 48 (2011) 1409–1416, https://doi.org/10.1016/j.bone.2011.03.675.
[36] I.-H. Song, A.I. Caplan, J.E. Dennis, In vitro dexamethasone pretreatment enhances bone formation of human mesenchymal stem cells in vivo, J. Orthop. Res.: official publication of the Orthopaedic Research Society 27 (2009) 916–921, https://doi.org/10.1002/jor.20838.
[37] F. Langenbach, K. Berr, C. Naujoks, A. Hassel, M. Hentschel, R. Depprich, N.R. Kubler, U. Meyer, H.-P. Wiesmann, G. Kögler, J. Handschel, Generation and differentiation of microtissues from multipotent precursor cells for use in tissue engineering, Nat. Protoc. 6 (2011) 1726–1735, https://doi.org/10.1038/nprot.2011.394.
[38] S.N. Tzouanas, A.K. Ekenseair, F.K. Kasper, A.G. Mikos, Mesenchymal stem cell and gelatin microparticle encapsulation in thermally and chemically gelling injectable hydrogels for tissue engineering, J. Biomed. Mater. Res. 102 (2014) 1222–1230, https://doi.org/10.1002/jbm.a.35093.
[39] A. Linde, A. Lussi, M.A. Crenshaw, Mineral induction by immobilized polyanionic proteins, Calcif. Tissue Int. 44 (1989) 286–295, https://doi.org/10.1007/BF02553763.
[40] R.W. Romberg, P.G. Werness, B.L. Riggs, K.G. Mann, Inhibition of hydroxyapatite crystal growth by bone-specific and other calcium-binding proteins, Biochemistry 25 (1986) 1176–1180, https://doi.org/10.1021/bi00353a035.
[41] H.A. Goldberg, K.J. Warner, M.J. Stillman, G.K. Hunter, Determination of the hydroxyapatite-nucleating region of bone sialoprotein, Connect. Tissue Res. 35 (1996) 385–392, https://doi.org/10.3109/03008209609029216.
[42] G.K. Hunter, H.A. Goldberg, Nucleation of hydroxyapatite by bone sialoprotein, Proc. Natl. Acad. Sci. U.S.A. 90 (1993) 8562–8565, https://doi.org/10.1073/pnas.90.18.8562.
[43] S. Eiden-Aßmann, M. Viertelhaus, A. Heiß, K. Hoetzer, J. Felsche, The influence of amino acids on the biomineralization of hydroxyapatite in gelatin, J. Inorg. Biochem. 91 (2002) 481–486, https://doi.org/10.1016/S0162-0134(02)00481-6.
[44] S.L. Ishaug-Riley, G.M. Crane, A. Gurlek, M.J. Miller, A.W. Yasko, M.J. Yaszemski, A.G. Mikos, Student research award in the doctoral degree candidate category, Society for Biomaterials 23rd Annual Meeting, New Orleans, LA, April 30-May 4, 1997: ectopic bone formation by marrow stromal osteoblast transplantation using poly(DL-lactic-co-glycolic acid) foams implanted into the rat mesentery, J. Biomed. Mater. Res. 36 (1997) 1–8, https://doi.org/10.1002/(sici)1097-4636(199707)36:1<1:aid-jbm1>3.0.co;2-p.
[45] M. Knippenberg, M.N. Helder, B. Zandieh Doulabi, P.I.J.M. Wuisman, J. Klein-Nulend, Osteogenesis versus chondrogenesis by BMP-2 and BMP-7 in adipose stem cells, Biochem. Biophys. Res. Commun. 342 (2006) 902–908, https://doi.org/10.1016/j.bbrc.2006.02.052.
[46] A.M. Bratt-Leal, A.H. Nguyen, K.A. Hammersmith, A. Singh, T.C. McDevitt, A microparticle approach to morphogen delivery within pluripotent stem cell aggregates, Biomaterials 34 (2013) 7227–7235, https://doi.org/10.1016/j.biomaterials.2013.05.079.
[47] A.K. Kudva, A.D. Dikina, F.P. Luyten, E. Alsberg, J. Patterson, Gelatin microspheres releasing transforming growth factor drive in vitro chondrogenesis of human periosteum derived cells in micromass culture, Acta Biomater. 90 (2019) 287–299, https://doi.org/10.1016/j.actbio.2019.03.039.
[48] L. Nguyen, S. Bang, I. Noh, Tissue regeneration of human mesenchymal stem cells on porous gelatin micro-carriers by long-term dynamic in vitro culture, Tissue Eng. Regenerative Med. 16 (2019) 19–28, https://doi.org/10.1007/s13770-018-00174-8.
[49] A.H. Reddi, Interplay between bone morphogenetic proteins and cognate binding proteins in bone and cartilage development: noggin, chordin and DAN, Arthritis Res. 3 (2001) 1–5, https://doi.org/10.1186/ar133.
[50] E. Gazzerro, E. Canalis, Bone morphogenetic proteins and their antagonists, Rev. Endocr. Metab. Disord. 7 (2006) 51–65, https://doi.org/10.1007/s11154-006-9000-6.
[51] K. Schwabe, A. Ewe, C. Kohn, T. Loth, A. Aigner, M.C. Hacker, M. Schulz-Siegmund, Sustained delivery of siRNA poly- and lipopolyplexes from porous macromer-crosslinked gelatin gels, Int. J. Pharm. 526 (2017) 178–187, https://doi.org/10.1016/j.ijpharm.2017.04.065.
[52] A. Saparov, V. Ogay, T. Nurgozhin, M. Jumabay, W.C.W. Chen, Preconditioning of human mesenchymal stem cells to enhance their regulation of the immune response, Stem Cell. Int. 2016 (2016) 3924858, https://doi.org/10.1155/2016/3924858.
[53] D. García-Sánchez, D. Fernández, J.C. Rodríguez-Rey, F.M. Pérez-Campo, Enhancing survival, engraftment, and osteogenic potential of mesenchymal stem cells, World J. Stem Cell. 11 (2019) 748–763, https://doi.org/10.4252/wjsc.v11.i10.748.
[54] S. Schulze, D. Wehrum, P. Dieter, U. Hempel, A supplement-free osteoclast-osteoblast co-culture for pre-clinical application, J. Cell. Physiol. 233 (2018) 4391–4400, https://doi.org/10.1002/jcp.26076.